Journal of Southeast University (English Edition) Vol. 23, No. 2, pp. 278 – 284 June 2007 ISSN 1003—7985

Numerical study of forward smoldering combustion of polyurethane foam

Jia Baoshan[1,2] Xie Maozhao[1]

([1] School of Energy and Power Engineering, Dalian University of Technology, Dalian 116024, China)

([2] School of Safety Science and Engineering, Liaoning Technical University, Fuxin 123000, China)

Abstract: A two-dimensional and two-phase numerical model is presented for the smolder propagation in a horizontal polyurethane foam. The chemical processes considered include endothermic pyrolysis and exothermic oxidation degradation of polyurethane foam and exothermic oxidation of char. The governing equations are discretized in space using the finite element method and solved by the software package FEMLAB. Predicted profiles of solid temperature as well as evolutions of solid compositions (including foam, char and ash) are presented at an airflow velocity of 0.28 cm/s. The computed average smoldering velocity is 0.021 4 cm/s, and the average maximum temperature is 644.67 K. Based on the evolutions of solid compositions, the packed bed can be obviously divided into four zones: unreacted zone, fuel pyrolysis and oxidation zone, char oxidation zone and fuel burned-out zone. Simultaneously, the effects of inlet air velocity and fuel properties (including thermal conductivity, specific heat, density and pore diameter) are studied on the smoldering propagation. The results show that the smoldering velocity and temperature have a roughly linear increase with increasing inlet air velocity; the fuel density is the most important factor in determining smoldering propagation; radiation has a non-negligible role on the smoldering velocity for larger pore diameters of porous material. The computational results are compared with the experimental data and a general agreement is reached.

Key words: polyurethane foam; forward smoldering; porous medium; smoldering velocity; numerical study

Smoldering combustion is defined as a heterogeneous, surface combustion reaction without flame in the interior of a porous medium[1]. Compared with the flaming combustion, the smoldering combustion occurs at relatively low temperatures and very small velocities. For a smoldering wave to propagate, a sufficient heat amount must be transferred from the exothermic reactions to the fresh fuel ahead to bring its temperature to a level high enough to initiate the surface combustion reaction. Simultaneously, sufficient oxygen must also be transported to the reaction zone from the outside to sustain the reaction. Therefore, the fuel must be sufficiently porous, so that the smoldering wave can propagate through the interior of porous media[2].

Smoldering combustion is generally classified into forward and/or reverse configurations. In forward smolder, the reaction zone propagates in the same direction as the inlet airflow. In reverse smolder, the fresh airflow enters the reaction zone from the opposite direction of smoldering wave propagation[3]. The forward smolder is unsteady and moves at a higher rate, and can eventually transit to flaming combustion as the smoldering velocity increases due to the increased inlet air velocity or oxygen concentration[4]. The reverse smolder is characterized by a steady propagation velocity and cannot transit into flaming.

In comparison with other combustion processes, a relatively small amount of fundamental work has been done to date on smoldering combustion. During the last two decades, smoldering combustion has been previously studied numerically, analytically and experimentally. Most of the experimental analyses have focused on measuring the smoldering velocity under forced airflow conditions. Ohlemiller provided two thorough reviews[5-6] of experimental and theoretical studies present in the literature.

In this paper, based on the previous studies mentioned above, the propagation process of forward smoldering is numerically simulated and theoretically analyzed for polyurethane foam.

1 Physical-Chemical Model

So far, the smolder mechanism has been theoretically studied mostly by using a one-step or a two-step kinetics model. However, Kashiwagi et al.[7-8] em-

Received 2007-03-07.

Foundation item: The National Natural Science Foundation of China (No. 50476073).

Biographies: Jia Baoshan (1972—), male, graduate, associate professor, jiabaoshan72918@sina.com.cn; Xie Maozhao (corresponding author), male, professor, xmz@dlut.edu.cn.

ployed a three-step reaction model to study smolder combustion experimentally and theoretically. The total smolder process includes endothermic pyrolysis of fuel, exothermic oxidation of fuel and exothermic char oxidation. In this paper, the smolder characteristics are analytically studied for porous materials based on this model, and the model configuration of a fuel packed bed is shown in Fig. 1.

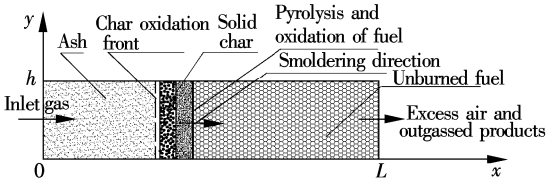

Fig. 1 Schematic diagram of forward smolder

The packed bed of polyurethane foam is 800 mm wide and 60 mm high. The inlet airflow is forced into the fuel bed from the left side, and the hot airflow and gaseous products (including H_2O, CO, and CO_2) exit from the right side. The smolder direction is from left to right, namely forward smolder.

The reactions between solid and gas taking place in the packed bed of porous polyurethane foam include the following three steps:

① Endothermic pyrolysis of fuel:

$$\text{Fuel} \longrightarrow n_{\text{C},1}\text{Char} + n_{\text{CO},1}\text{CO} + n_{\text{CO}_2,1}\text{CO}_2 + n_{\text{H}_2\text{O},1}\text{H}_2\text{O} \qquad -\Delta h_1$$

② Exothermic oxidation of fuel:

$$\text{Fuel} + n_{\text{O},2}\text{O}_2 \longrightarrow n_{\text{C},2}\text{Char} + n_{\text{CO},2}\text{CO} + n_{\text{CO}_2,2}\text{CO}_2 + n_{\text{H}_2\text{O},2}\,\text{H}_2\text{O} \qquad +\Delta \text{h}_2$$

③ Exothermic oxidation of char:

$$\text{Char} + n_{\text{O},3}\text{O}_2 \longrightarrow n_{\text{A},3}\,\text{Ash} + n_{\text{CO},3}\text{CO} + n_{\text{CO}_2,3}\text{CO}_2 + n_{\text{H}_2\text{O},3}\text{H}_2\text{O} \qquad +\Delta h_3$$

where $n_{j,i}(j = \text{CO, O, CO, CO}_2, \text{H}_2\text{O, A}; i = 1, 2, 3)$ denotes stoichiometric coefficients (mass fraction) of species in the three reactions, respectively; and Δh_i denotes the enthalpy of reactions. The stoichiometric coefficients are listed in Tab. 1 taken from Ref. [7].

Tab. 1 Stoichiometric coefficients (by mass fraction)

Fuel pyrolysis		Fuel oxidation		Char oxidation	
Coefficient	Value	Coefficient	Value	Coefficient	Value
$n_{\text{O}_2,1}$	0.00	$n_{\text{O}_2,2}$	0.41	$n_{\text{O}_2,3}$	1.65
$n_{\text{C},1}$	0.46	$n_{\text{C},2}$	0.29	$n_{\text{A},3}$	0.05
$n_{\text{CO},1}$	0.01	$n_{\text{CO},2}$	0.08	$n_{\text{CO},3}$	0.50
$n_{\text{CO}_2,1}$	0.03	$n_{\text{CO}_2,2}$	0.24	$n_{\text{CO}_2,3}$	1.80
$n_{\text{H}_2\text{O},1}$	0.50	$n_{\text{H}_2\text{O},2}$	0.80	$n_{\text{H}_2\text{O},3}$	0.30

All the processes mentioned above are described by a single first-order reaction with Arrhenius temperature dependency[9]:

$$r_1 = A_1 \exp\left(-\frac{E_1}{RT_s}\right)\rho_{\text{F}} \tag{1}$$

$$r_2 = A_2 \exp\left(-\frac{E_2}{RT_s}\right)\rho_{\text{F}}\rho_{\text{O}_2} \tag{2}$$

$$r_3 = A_3 \exp\left(-\frac{E_3}{RT_s}\right)\rho_{\text{C}}\rho_{\text{O}_2} \tag{3}$$

where r_i is the reaction rate of the i-th reaction ($i = 1, 2, 3$), A_i is the pre-exponential frequency factor of the i-th reaction, E_i is the activation energy, R is the universal gas constant, T_s is the solid temperature, ρ_{F} is the density of fuel, ρ_{C} is the density of char, and ρ_{O_2} is the density of O_2.

2 Numerical Model of Smolder

In developing the governing transport equations, the appropriate assumptions are made as follows:

① The fluid flow, and heat and mass transfer are time dependent, two-dimensional and laminar.

② The thermo-physical properties of the condensed phase (including foam, char and ash) and fluid are homogeneous and isotropic, and the chemical properties (including action energy, pre-exponential frequency factor, enthalpy, etc) remain constant during smolder.

③ The cavities of the porous matrix are spherical and are saturated with fluid and the phases present in any small volume elements are in thermal equilibrium.

④ The porous matrix is rigid and incompressible, while volumetric change due to the change of phase and chemical reaction is permitted.

⑤ The heat quantity only results from oxidation reaction. There is not any source of volumetric heat in the packed bed.

⑥ The process of ignition for the fuel-packed bed is simulated by setting the boundaries and initial conditions.

⑦ The gas mixture satisfies the state equation. The specific heat of species is equal and constant, and the Lewis number, *Le*, is 1.

The smolder of porous fuel is a two-phased process (including solid and gas) flow with chemical reactions. Based on the above assumptions, we can express the governing equations of the problem as follows.

2.1 Solid-phase continuity equations

$$\frac{\partial}{\partial t}[(1-\varphi)\rho_{\text{F}}] = -r_1 - r_2 \tag{4}$$

$$\frac{\partial}{\partial t}[(1-\varphi)\rho_{\text{C}}] = n_{\text{C},1}r_1 + n_{\text{C},2}r_2 - r_3 \tag{5}$$

$$\frac{\partial}{\partial t}[(1-\varphi)\rho_A] = n_{A,3} r_3 \quad (6)$$

where φ is the porosity of the polyurethane foam packed bed.

2.2 Gas-phase continuity equations

$$\frac{\partial \varphi \rho_g}{\partial t} + \nabla \cdot (\varphi \rho_g \nu) = (1 - n_{C,1}) r_1 + (1 + n_{O_2,2} - n_{C,2}) r_2 + (1 + n_{O_2,3} - n_{A,3}) r_3 \quad (7)$$

where ρ_g is the density of gas, v is the gas velocity through the polyurethane foam along the packed bed, and r_j is reaction rate $(j = 1, 2, 3)$.

2.3 Gas species equations

$$\frac{\partial \varphi \rho_g Y_i}{\partial t} + \nabla \cdot (\varphi \rho_g \nu Y_i) = \Omega_i + \nabla \cdot (\varphi \rho_g D \nabla Y_i) \quad (8)$$

where $\Omega_i = \sum_{j=1}^{3} \pm n_{i,j} r_j (i = O_2, CO, CO_2, H_2O; j = 1, 2, 3)$; $n_{i,j}$ are the stoichiometric coefficients (mass fraction) of species in the three reactions, respectively; Y_i is the mass fraction of gaseous species. The minus sign (−) is for consumed gas species; the plus sign (+) is for generated species.

In addition, since the transport of oxygen to the burning front depends critically on its ability to diffuse through the gas phase, it is important to include a correct dependence of diffusivity on temperature[10]. The diffusion coefficient D is expressed as

$$D = 0.677 D_g \varphi^{1.18} \left(\frac{T_g}{273}\right)^{1.75}$$

where D_g is the unrestrained diffusion of gas in a binary mixture, and T_g is the temperature of the gas phase.

2.4 Energy equations

$$\frac{\partial}{\partial t}[(1-\varphi)(\rho_F h_F + \rho_C h_C + \rho_A h_A)] = \nabla \cdot [(1-\varphi)\lambda_{eff} \nabla T_s] + \sum_{i=1}^{3} r_i \Delta h_i + h A_s (T_g - T_s) \quad (9)$$

$$\frac{\partial}{\partial t}(\varphi \rho_g h_g) + \nabla \cdot (\varphi \rho_g \nu h_g) = \nabla \cdot (\varphi \lambda_g \nabla T_g) + h A_s (T_s - T_g) \quad (10)$$

where h_F, h_C, h_A and h_g are the specific enthalpy per unit mass of fuel, char, ash and gas, respectively; $h_F = C_F(T_s - T_\infty)$, $h_C = C_C(T_s - T_\infty)$, $h_A = C_A(T_s - T_\infty)$, $h_g = C_g(T_g - T_\infty)$; C_F, C_C, C_A and C_g are the specific heat of fuel, char, ash and gas, respectively; T_s is the temperature of the solid phase; T_∞ is the ambient temperature, normally 300 K; T_g is the temperature of the gaseous phase; h is the convective transfer coefficient between the solid-phase and the gas-phase; A_s is the specific interfacial gas-solid surface and $A_S = 4(1-\varphi)/d$[11]; λ_{eff} is the effective heat conductivity of the porous medium and $\lambda_{eff} = (1-\varphi) k_s + 16\delta d T_s^3/3$[12]; k_s is the thermal conductivity of solid; d is the pore diameter; δ is the Stefan-Boltzmann constant.

2.5 State equation of gas

$$p = \frac{\rho_g R T_g}{M_{mix}} \quad (11)$$

where M_{mix} is the molecular weight of the gas mixture and $M_{mix}^{-1} = \sum \frac{Y_i}{M_i}$ $(i = O_2, CO, CO_2, N_2, H_2O)$; Y_i is the mass fraction of the gaseous species and $Y_{N_2} = 1 - Y_{CO} - Y_{CO_2} - Y_{O_2} - Y_{H_2O}$, $\sum Y_i = 1$; M_i is the molecular weight of the i-th gaseous species.

In this model, the simulated polyurethane foam is highly porous ($\varphi = 0.975$), and the pressure drop across the porous medium is trivial[19]. Therefore, the conservation of momentum equations can be negligible. The gas velocity in the porous medium is solved directly by using the overall continuity equation and Eq. (11). Thus we have totally 10 unknown parameters as follows: ρ_g, Y_{CO}, Y_{CO_2}, Y_{O_2}, Y_{H_2O}, T_s, T_g, ρ_F, ρ_C, and ρ_A.

There are ten independent equations, thus the problem is closed and can be solved.

3 Boundary and Initial Conditions

The computed domain is shown in Fig. 1. Airflow is forced into the fuel packed bed from the left side, and the hot gases, including generated gaseous species, exit from the right side. The smolder propagation direction is also from left to right through the packed bed, namely forward smolder.

3.1 Boundary conditions

1) At the left boundary $x = 0$, all the parameters are specified as $T_{gin} = 300$, $Y_{O_2} = 0.23$, $Y_{CO_2} = 3.2 \times 10^{-4}$, $Y_{CO} = 0$, $Y_{H_2O} = 0.002$, $v_x(0, y, t) = 0.28$, $v_y(0, y, t) = 0$, $\nabla \rho_j = 0 (j = F, C, A)$, $\nabla Y_i = 0 (i = CO, CO_2, H_2O, O_2)$, $\rho_g = 1.164$.

The ignition temperature is fixed at 900 K for 60 s and the smolder wave is assumed to start to propagate along the packed bed. Thus the process of ignition is simulated as

$$T_s(0, y, t) = \begin{cases} 900 & t < 60 \\ 300 & t \geqslant 60 \end{cases}$$

2) At the right boundary $x = L$, the hot gases exit and the gradients of parameters are assumed to be zero: $\nabla T_s = 0$, $\nabla T_g = 0$, $\nabla \rho_g = 0$, $\nabla Y_i = 0 (i = CO, CO_2, H_2O, O_2)$, $\nabla \rho_j = 0 (j = F, C, A)$.

3) At the bottom and top surfaces, the walls are assumed to be thermally insulated.

3.2 Initial condition

At $t=0$, the entire fuel bed is unreacted. All parameters (including temperature, gas species, solid density) are given: $T_{s0}=300$, $T_{g0}=300$, $Y_{O_2}=0.23$, $\rho_{A0}=0$, $Y_{CO}=Y_{CO_2}=Y_{H_2O}=0$, $\rho_{F0}=26.5$, $\rho_{C0}=0$, $\rho_{g0}=1.164$, $v_{x0}=0.28$, $v_{y0}=0$.

4 Numerical Results

As shown in Fig. 2, the packed bed is divided into 960 meshes to perform calculations. The governing equations are solved using FEMLAB 3.1 which is a software package using numerical techniques based on the finite element method for the spatial discretization. Fuel properties are chosen from Refs. [7−8] and listed in Tab. 2.

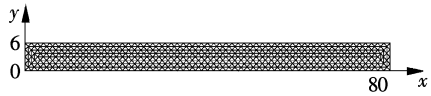

Fig. 2 Computed meshes (unit: cm)

Tab. 2 Properties of fuel

Parameters	Value	Parameters	Value
$E_1/(\mathrm{kJ\cdot mol^{-1}})$	220	$\varphi/\%$	97.5
$E_2/(\mathrm{kJ\cdot mol^{-1}})$	160	$\mu_g/(\mathrm{kg\cdot(m\cdot s)^{-1}})$	3×10^{-5}
$E_3/(\mathrm{kJ\cdot mol^{-1}})$	160	$\Delta h_1/(\mathrm{kJ\cdot kg^{-1}})$	−570
$A_1/\mathrm{s^{-1}}$	2.0×10^{17}	$\Delta h_2/(\mathrm{kJ\cdot kg^{-1}})$	5 700
$A_2/(\mathrm{s^{-1}\cdot m^3\cdot kg^{-1}})$	5.7×10^{11}	$\Delta h_3/(\mathrm{kJ\cdot kg^{-1}})$	25 000
$A_3/(\mathrm{s^{-1}\cdot m^3\cdot kg^{-1}})$	5.0×10^{8}	$D/(\mathrm{m^2\cdot s^{-1}})$	4.5×10^{-5}
$C_F/(\mathrm{kJ\cdot(kg\cdot K)^{-1}})$	1.7	d_p/m	5.0×10^{-4}
$C_C/(\mathrm{kJ\cdot(kg\cdot K)^{-1}})$	1.1	d/m	1.0×10^{-4}
$C_A/(\mathrm{kJ\cdot(kg\cdot K)^{-1}})$	1.1	$h/(\mathrm{W\cdot(m^2\cdot K)^{-1}})$	5.85
$C_g/(\mathrm{kJ\cdot(kg\cdot K)^{-1}})$	1.1	$\rho_{ref}/(\mathrm{kg\cdot m^{-3}})$	1.2
$k_g/(\mathrm{W\cdot(m\cdot K)^{-1}})$	0.025 8	T_∞/K	300
$K_s/(\mathrm{W\cdot(m\cdot K)^{-1}})$	0.063 0		

4.1 Distribution of solid temperature

The profiles of solid temperature at different times are shown in Fig. 3. Each curve represents a different time step and results are plotted in increments of approximate 450 s. Initially, the solid is at 300 K. Airflow is forced through the left boundary into the packed bed with a velocity of 0.28 cm/s.

As shown in Fig. 3, in the initial stage of smolder, the solid temperature is rather high (about 760 K) due to the influence of ignition at the left boundary. With the development of smolder, the distribution of solid temperature is driven to stabilization and the average maximum temperature is about 644.67 K. The average smoldering velocity, measured by the ratio of the propagation distance of the smolder wave peak to experienced time, is about 0.021 4 cm/s in this case.

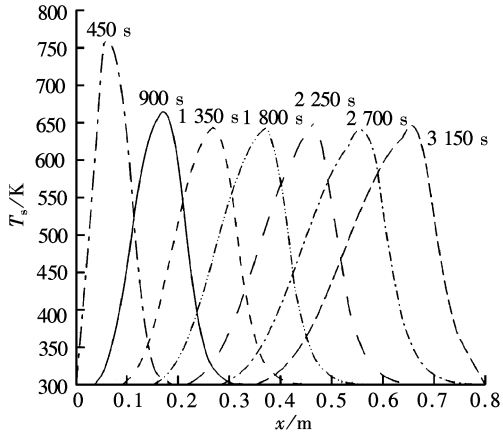

Fig. 3 Profiles of solid temperature at different times

The curve of solid temperature presents a parabolic shape. First, the fuel is heated by conduction, convection and radiation, whose temperature gradually rises. In the reaction zone, the temperature reaches the maximum value because of exothermic oxidation reaction. Then, with the movement of the smolder wave, the temperature gradually recovers the initial value (300 K). Moreover, the profiles of solid temperature at different locations are plotted in Fig. 4.

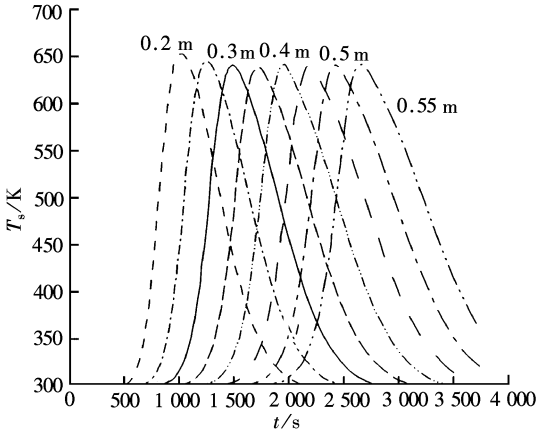

Fig. 4 Profiles of solid temperature at different locations

4.2 Evolutions of solid compositions

In Fig. 5, the evolutions of solid compositions (including foam, char and ash) are presented along the fuel packed bed at 2200s ($x=407$ cm). The packed bed can be obviously divided into four zones: unreacted zone ($x>0.472$), fuel pyrolysis and oxidation zone ($0.367<x<0.472$), char oxidation zone ($0.261<x<0.367$) and burned-out zone ($x<0.261$).

At the unreacted zone, the density of fuel remains at its original value of 26.5 kg/m^3. At the zone of fuel pyrolysis and oxidation, the pyrolysis and oxidation reactions of fuel take place simultaneously. Some chars come into being during the two reactions and their density increases from 0 to 17.32 kg/m^3. The fuel density decreases from 26.5 to 1.75 kg/m^3 due to the con-

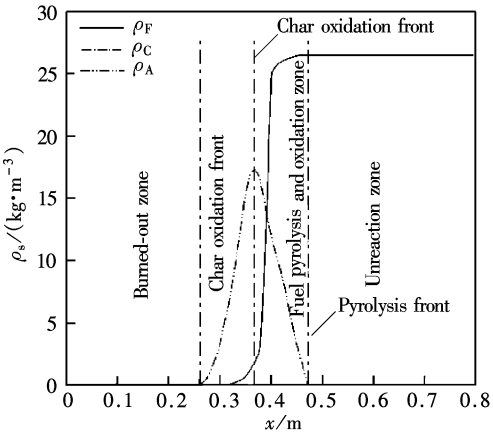

Fig. 5 Evolutions of solid compositions ($x = 0.407$ m)

sumption.

At the char oxidation zone, char is further oxidized into ash whose density increases from 0 to 0.95 kg/m^3, while the density of char decreases from 17.32 kg/m^3 to 0. Finally, at burned-out zero, there is only ash left as a residual solid product that does not react anymore.

When the inlet air velocity is 0.28 cm/s, the pyrolysis front of fuel moves faster so it is 0.105 m ahead of the oxidation front of char. The distance between the two fronts will decrease with the increase in inlet air velocity. The variation trend results from greatly accelerating char oxidation owing to abundant oxygen supply. Moreover, at the char oxidation zone, there is a little unburned fuel left whose density varies from 1.75 kg/m^3 to 0. It is verified that the three reactions (including pyrolysis, fuel oxidation and char oxidation) simultaneously happen when the smolder wave is propagating forward.

4.3 Effect of inlet air velocity on smolder

In order to compare with experimental results measured by Torero et al.[1], corresponding inlet air velocities (including 0.09, 0.17, 0.28, 0.41, 0.53, and 0.78 cm/s) were used in the simulation. The effect of inlet air velocity is examined on the smoldering velocity of polyurethane foam. As shown in Fig. 6, the computed and experimental smoldering velocity as a function of inlet air velocity is presented, and the numerical smoldering velocity simulated of Leach et al.[13] is also plotted. All the results show a roughly linear relationship between smoldering velocity and inlet air velocity. The reason is that increasing airflow makes the oxidation reactions occur more rapidly, and the fuel combusts more completely, and the smoldering velocity propagates faster. The computed velocities agree very well with the measurements of Torero et al.[1] and the simulated results of Leach et al.[13].

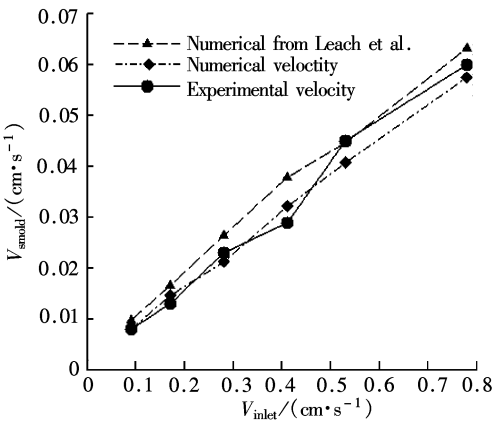

Fig. 6 Relationship between the inlet air and smoldering velocity

In Fig. 7, the effect of inlet air velocity on the average maximum temperature is presented. It appears that the maximum temperature has a linear increase by increasing the inlet air velocity. Changing the inlet air velocity by a factor of 8.67 cm/s from 0.09 to 0.78 cm/s increases the maximum temperature by a factor of 1.14 from 628.29 to 719.03 K. The experimental data are derived from Ref. [1]. The calculated temperature also agrees with the experimental value.

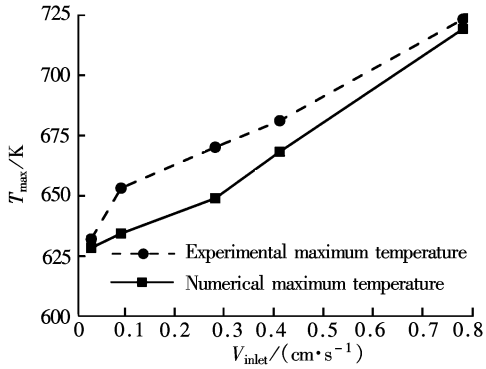

Fig. 7 Relationship between the inlet air velocity and the maximum temperature of smoldering

4.4 Effect of conductivity on smolder

All the parameters for the base case are changeless and the thermal conductivity of fuel λ_F is varied from 0.047 to 0.20 W/(m·K). The simulated results are listed in Tab. 3. Although changing the thermal conductivity of fuel by a factor of 4.3, the smoldering velocity basically remains constant between 0.022 and 0.021 cm/s and the maximum temperature of smolder varies only between 645 and 643 K. But the smoldering velocity and maximum temperature have a slight decrease because increasing conductivity can induce more heat

Tab. 3 Effect of conductivity

Number	$\lambda_F/(W\cdot(m\cdot K)^{-1})$	$V_{smold}/(cm\cdot s^{-1})$	T_{max}/K
1	0.047	0.021 57	644.95
2	0.063	0.021 50	644.67
3	0.085	0.021 36	643.16
4	0.113	0.021 40	643.30
5	0.200	0.020 80	642.93

loss from the reaction zone. In general, the thermal conductivity of fuel has little effect on the smoldering propagation.

4.5 Effect of fuel density on smolder

The density of fuel ρ_F is changed from 0.012 4 to 34 kg/m^3. As shown in Tab. 4, the simulations indicate that increasing the fuel density can decrease the smoldering velocity. When the smoldering velocity varies by a factor of 1.4 from 0.024 to 0.017 cm/s, the maximum temperature of fuel smolder decreases by only about 15 K. Compared to the conductivity of fuel, the fuel density has a greater effect on the smoldering velocity and has a certain effect on the maximum temperature.

Tab. 4 Effect of fuel density

Number	ρ_F/(kg·m^{-3})	V_{smold}/(cm·s^{-1})	T_{max}/K
1	0.012 4	0.023 7	665.84
2	0.15	0.022 9	656.23
3	0.5	0.021 8	649.22
4	26.5	0.021 4	644.67
5	34.0	0.016 8	641.35

4.6 Effect of specific heat on smolder

The specific heat of fuel C_F is chosen as: 0.5, 0.84, 1.7, 2.5, 3.4 kJ/(kg·K). The simulated results are presented in Fig. 8. It appears that changing the specific heat of fuel from 0.5 to 3.4 kJ/(kg·K) decreases the smoldering velocity from 0.023 2 to 0.019 4 cm/s, and the maximum temperature of smolder also decreases from 660.70 to 596.08 K. The reason is that increasing the specific heat results in an increase in heat absorption used to maintain smoldering propagation. Therefore, the smoldering velocity and maximum temperature of smolder have a certain decrease.

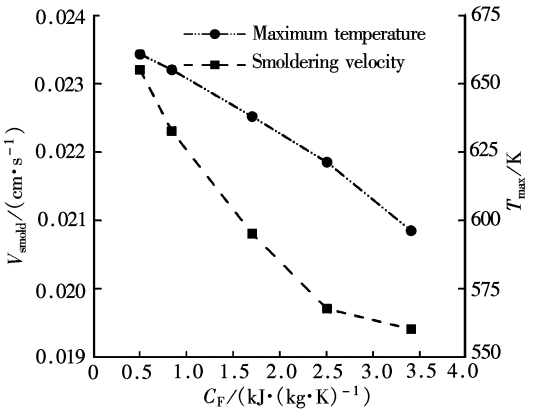

Fig. 8 Specific heat of fuel on smoldering characteristics

4.7 Effect of pore diameter

The pore diameter mainly affects both convective and radiative heat transfer. Increasing the pore diameter can effectively decrease the volumetric heat transfer coefficient by decreasing the area to volume ratio and increase the radiative conductivity. In order to qualitatively examine the effects of the pore diameter, different values of pore diameter (including 0.05, 0.1, 5 mm) are used to conduct simulations. Moreover, two different cases, with or without radiation, are taken into account. The results are summarized in Tab. 5.

Tab. 5 Effect of pore diameter

Number	D/mm	V_{smold}/(cm·s^{-1})	T_{max}/K	Radiation
1	0.05	0.021 2	643.56	Yes
		0.021 2	643.77	No
2	0.10	0.021 4	644.67	Yes
		0.021 3	645.02	No
3	5.00	0.022 3	646.09	Yes
		0.021 8	646.78	No

When the pore diameter is very small, such as 0.005 cm, radiation is not important. The smoldering velocity is the same (0.021 2 cm/s) and the maximum temperature of smolder remains almost constant (644 K). So radiation can be neglected for studying smoldering propagation in porous material with small pore diameters, and heat is transferred mainly by convection and conduction. When the pore diameter is 0.1 mm, the smoldering velocity will increase. Radiation has a certain effect on the smoldering velocity. Increasing pore diameter can enhance the radiation, and the smoldering velocity also accelerates. The maximum temperature will decrease with radiation in this case due to the heat emitting from the reaction. When the pore diameter is larger (5 mm), radiation has an important effect on the smoldering velocity and the maximum temperature. So radiation heat transfer for larger pore diameters of porous material is not negligible.

5 Conclusions

1) A two-dimensional, unsteady, numerical model is presented for the forward smolder in horizontal polyurethane foam by using a three-step kinetics mechanism. It provides a basis for further detailed study of smoldering propagation in a porous medium.

2) The distribution of solid compositions is simulated along the packed bed. There are four zones: unreacted zone, fuel pyrolysis and oxidation zone, char oxidation zone and burned-out zone. It is easier to understand the three-step kinetic mechanism. The distance between the pyrolysis front and char oxidation front will shorten with increasing inlet air velocity due to acceleration of char oxidation.

3) By varying the properties of fuel (including thermal conductivity, specific heat, and density), the simulations indicate that the fuel density is the most

important and fuel conductivity is the least important factor affecting the smoldering velocity and the maximum temperature of fuel. The specific heat has a certain effect on smolder propagation.

4) Radiation is not important and can be neglected for small pore diameters of porous materials. However, radiation has a non-negligible role on the smoldering velocity for larger pore diameters of porous materials.

References

[1] Torero J L, Fernandez-Pello A C. Forward smolder of polyurethane foam in a forced air flow [J]. *Combustion and Flame*, 1996, **106**(1/2): 89 - 109.

[2] Krause U, Schmidt M, Lohrer C. A numerical model to simulate smoldering fires in bulk materials and dust deposits [J]. *Journal of Loss Prevention in the Process Industries*, 2006, **19**(2/3): 218 - 226.

[3] Wang J H, Chao C Y H, Kong W J. Experimental study and asymptotic analysis of horizontally forced forward smoldering combustion[J]. *Combustion and Flame*, 2003, **135**(4): 405 - 419.

[4] Aldushin A P, Bayliss A, Matkowsky B J. On the transition from smoldering to flaming[J]. *Combustion and Flame*, 2006, **145**(3): 579 - 606.

[5] Ohlemiller T J, Locca D A. An experimental comparison of forward and reverse smolder propagation in permeable fuel [J]. *Combustion and Flame*, 1983, **54**(1/2/3): 131 - 147.

[6] Ohlemiller T J. Modeling of smolder combustion propagation [J]. *Progress in Energy and Combustion Science*, 1985, **11**(4): 277 - 310.

[7] Kashiwagi T, Nambu H. Global kinetic constants for thermal oxidative degradation of a cellulosic paper [J]. *Combustion and Flame*, 1992, **88**(3/4): 345 - 368.

[8] Rogers F E, Ohlemiller T J. Smolder characteristics of flexible polyurethane foams [J]. *Fire and Flammability*, 1980, **11**(1): 32 - 44.

[9] Di Blasi C. Mechanisms of two-dimensional smoldering propagation through packed beds [J]. *Combustion Science and Technology*, 1995, **106**(1/2/3): 103 - 124.

[10] Rostami A, Murthy J, Hajaligol M. Modeling of a smoldering cigarette [J]. *Journal of Analytical and Applied Pyrolysis*, 2003, **66**(1/2): 281 - 301.

[11] Xie Maozhao, Liang Xiaohong. Numerical simulation of combustion and ignition-quenching behavior of a carbon packed bed [J]. *Combustion Science and Technology*, 1997, **125**(1/2/3/4/5/6): 1 - 24.

[12] Leach S V, Ellzey J L, Ezekoye O A. A numerical study of reverse smoldering [J]. *Combustion Science and Technology*, 1997, **130**(1/2/3/4/5/6): 247 - 267.

[13] Leach S V, Rein G, Ellzey J L, et al. Kinetic and fuel property effects on forward smolder combustion [J]. *Combustion and Flame*, 2000, **120**(3): 346 - 358.

聚氨酯泡沫燃料正向阴燃传播特性的数值模拟

贾宝山[1,2]　　解茂昭[1]

([1] 大连理工大学能源与动力学院,大连 116024)

([2] 辽宁工程技术大学安全科学与工程学院,阜新 123000)

摘要: 以聚氨酯泡沫为试样,建立了多孔介质水平燃料床阴燃的二维两相流数学模型. 模型包括燃料吸热热解、燃料放热氧化及焦炭的放热氧化 3 个反应过程. 通过有限单元法对聚氨脂泡沫的阴燃控制方程进行离散,并采用数值分析软件包 FEMLAB 进行计算求解. 数值模拟了来流速度为 0.28 cm/s 时燃料阴燃的温度分布和固体成分(燃料泡沫、炭粒和灰分)的变化,其中阴燃传播平均速度为 0.0214 cm/s,阴燃最高温度平均为 644.67 K;固体成分的变化曲线明显的将填充床分成 4 个区域:未燃区、燃料热解氧化区、焦炭氧化区及燃料燃尽区. 同时,模拟研究了来流速度及燃料特性参数(导热率、比热、密度、孔隙直径等)对阴燃传播特性的影响. 结果表明:阴燃速度和阴燃温度随着来流速度的增大基本上呈线性增长;燃料密度对阴燃传播影响最大;对于孔径较大的多孔介质燃料,模型中要考虑辐射的影响. 模拟数据与实验数据进行了对比,结果基本吻合.

关键词: 聚氨酯泡沫;正向阴燃;多孔介质;阴燃速度;数值模拟

中图分类号: O642.1